7167-38179

CR - 72293

ELECTROCHEMICAL CHARACTERIZATION OF NON-AQUEOUS SYSTEMS FOR SECONDARY BATTERY APPLICATION

by

M. Shaw, O. A. Paez, R. J. Radkey, A. H. Remanick

prepared for

Ag/34c5⁴

P-1

Requests for copies of this report should be referred to

National Aeronautics and Space Administration
Scientific and Technical Information Division
Attention: USS-A
Washington, D. C. 20546

FIFTH QUARTERLY REPORT

ELECTROCHEMICAL CHARACTERIZATION
OF NON-AQUEOUS SYSTEMS
FOR SECONDARY BATTERY APPLICATION

May, 1967 - July, 1967

by

M. Shaw, O. A. Paez, R. J. Radkey, A. H. Remanick

prepared for

NATIONAL AERONAUTICS AND SPACE ADMINISTRATION

August 21, 1967

CONTRACT NAS 3-8509

NARMCO RESEARCH AND DEVELOPMENT DIVISION

OF

WHITTAKER CORPORATION
3540 Aero Court
San Diego, California 92123

TABLE OF CONTENTS

CYCLIC VOLTAMMOGRAMS

LIST OF TABLES

ELECTROCHEMICAL CHARACTERIZATION
OF NON-AQUEOUS SYSTEMS
FOR SECONDARY BATTERY APPLICATION

by

M. Shaw, O. A. Paez, R. J. Radkey, A. H. Remanick

ABSTRACT

Multisweep cyclic voltammograms have been obtained for an additional
153 systems comprising silver, copper, nickel, cobalt, zinc, cadmium,
molybdenum, indium, and iron electrodes in acetonitrile, butyrolactone,
dimethylformamide, and propylene carbonate solutions of chlorides,
perchlorates, and fluorides.

The effect of solute concentration and water impurity on the cyclic voltam-
mograms of a number of systems was determined.

Voltammograms are presented for thirty-one of these systems. Tabular
data includes peak current density, sweep index, anodic-to-cathodic peak
displacement, coulombic ratio, and discharge capacity. Systems exhibiting
no anodic or no cathodic peaks are listed, as well as those causing instru-
ment overload due to a combination of high current and relatively low
conductance.

SUMMARY

The electrochemical characterization of nonaqueous battery systems by
multisweep cyclic voltammetry has been continued. Cyclic voltammograms
are now available on nearly seven hundred systems comprising silver, copper,
nickel, cobalt, zinc, cadmium, molybdenum, indium, and iron in chloride,
perchlorate, and fluoride solutions of acetonitrile, butyrolactone, dimethyl-
formamide, and propylene carbonate. Solutes consist primarily of $AlCl_3$,
$LiCl$, $MgCl_2$, $Mg(ClO_4)_2$, $LiClO_4$, MgF_2, $LiPF_6$, $LiBF_4$, and KPF_6. The
voltammograms of thirty-one systems are included in this report.

During this reporting period, the effects of solute concentration and water
impurity on the cyclic voltammograms of a number of systems were deter-
mined. Solute concentrations were varied from 0.5 to 3.0 m. Water
addition varied from 500 to 2000 ppm. Cyclic voltammetry was initiated on
indium and iron electrodes. In general, iron electrodes exhibit low or
negligible electrochemical activity. When activity was indicated, it was
usually only anodic, with no cathodic current evident, which may have been
due to immediate dissolution of the anodic product. Indium electrodes show
promising electrochemical activity. Measurements were continued on metal
oxide, chloride, and fluoride electrodes.

Tables are presented listing system parameters derived from the cyclic
voltammograms. These tables include data on peak current densities, sweep
index, anodic to cathodic peak displacement, coulombic ratio, and discharge
capacity. Listed also are those systems exhibiting no anodic or cathodic
peaks, as well as those systems causing instrument overload.

INTRODUCTION

The purpose of this program is to conduct a molecular level screening by the cyclic voltammetric method on a large number of electrochemical systems in nonaqueous electrolytes, and to characterize them as to their suitability for use in high energy density secondary batteries.

Since the release and storage of energy in a battery is initiated at the molecular level of the reaction, and therefore dependent on the charge and mass transfer processes, it is essential that screening be conducted at this level, in order to eliminate those systems whose electrode processes are inadequate for secondary battery operation.

I. RESULTS

A. ANALYSIS OF CYCLIC VOLTAMMOGRAMS

Table I lists the conductivities of the solutions used in preparing the electro-chemical systems screened during this quarter. The systems screened are shown in Tables II and III. This represents a total of 153 systems. Curve analysis was accomplished by dividing all systems into two major groups:

1. Systems involving chloride and perchlorate electrolytes
2. Systems involving fluoride electrolytes

Each main group was then subdivided according to the identity of the working electrode. Each of these subgroups was further broken down according to the identity of the solvent portion of the solution. The cyclic voltammograms are then discussed in terms of the total solution. This classification facilitates data analysis, and has permitted a more significant correlation among the electrochemical systems.

Except in those cases where the metal is converted to a cathodic material prior to assembly in the measuring cell, the working electrode is the base metal itself. During the voltage sweep, the metal is oxidized to some anodic product which serves as the cathode subsequently reduced during the cathodic portion of the sweep. Each sweep cycle thus corresponds to a charge-discharge cycle. In the absence of complicating factors, it is assumed that chloride cathodes would be formed in chloride electrolytes, and fluoride cathodes in fluoride electrolytes.

Each cyclic voltammogram is identified by a CV number and labelled according to the electrochemical system, sweep rate, temperature, and zero reference, representing the open circuit voltage (ocv) of the working electrode with respect to the indicated reference electrode. The current axis is

in units of ma/cm^2, each unit being of variable scale depending on the X-Y recorder sensitivity setting. A maximum sensitivity of $0.1 \, ma/cm^2/cm$ division has been established to avoid exaggerating the current background of poor systems. The sweep is always in a clockwise direction, the potential becoming more positive to the right. Positive currents represent anodic (charge) reactions, and negative currents represent cathodic (discharge) reactions. The voltage axis units are relative to the ocv so that voltage units are in terms of electrode polarization.

For comparative purposes, current density magnitude is classified according to very high (more than $300 \, ma/cm^2$), high (100 - 300 ma/cm^2), medium high (50-100 ma/cm^2), medium low (10-50 ma/cm^2), low (1-10 ma/cm^2), and very low (less than $1 \, ma/cm^2$).

Analysis is based on the cyclic voltammograms obtained at the lowest sweep rate, 40 mv/sec, except where additional information is required from the higher sweep rate curves to aid in the analysis.

TABLE I

ELECTROLYTE CONDUCTIVITY*

Electrolyte	Molality m	Conductivity $ohm^{-1}cm^{-1}$
Acetonitrile-$LiPF_6$	0.5 (1)	4.4×10^{-2}
Acetonitrile-$LiClO_4$	0.75	3.0×10^{-2}
Dimethylformamide-$LiClO_4$	2.5	1.4×10^{-2}
	1.5	2.6×10^{-2}
	1.0	2.6×10^{-2}
	0.5	1.9×10^{-2}
Dimethylformamide-KPF_6	2.0	2.5×10^{-2}
	1.5	2.4×10^{-2}
	1.0	2.4×10^{-2}
	0.75	1.2×10^{-2}
	3.0	5.8×10^{-3}
Dimethylformamide-$LiClO_4$+ LiCl	0.75 (1)	2.1×10^{-2}
Dimethylformamide-$Mg(ClO_4)_2$	0.75	1.9×10^{-2}
Acetonitrile-$AlCl_3$ + LiCl	0.25 (2)	1.9×10^{-2}
Butyrolactone-$LiClO_4$	0.75	1.7×10^{-2}

(1)   Concentration with respect to each salt

(2)   0.25 m in $AlCl_3$, saturated with LiCl

*   In order of decreasing conductivity

TABLE I (Cont'd.)

Electrolyte	Molality m		Conductivity $ohm^{-1}cm^{-1}$
Acetonitrile-$LiBF_4$	0.5		1.6×10^{-2}
Acetonitrile-$AlCl_3$ + LiCl	0.25	(1)	1.5×10^{-2}
Acetonitrile-KPF_6	0.5		1.5×10^{-2}
Dimethylformamide-$AlCl_3$ + LiCl	0.5	(1)	1.0×10^{-2}
Dimethylformamide-LiCl	2.5		6.6×10^{-3}
	1.5		9.4×10^{-3}
	1.0		9.7×10^{-3}
	0.5		7.7×10^{-3}
Dimethylformamide-$LiPF_6$	0.5		9.0×10^{-3}
Propylene carbonate-$AlCl_3$ + LiCl	0.5	(1)	8.7×10^{-3}
Propylene carbonate-$LiPF_6$	0.5		7.5×10^{-3}
Dimethylformamide-$MgCl_2$	0.5		7.0×10^{-3}

(1)   Concentration with respect to each salt

(2)   0.25 m in $AlCl_3$, saturated with LiCl

*   In order of decreasing conductivity

TABLE I (Cont'd.)

Electrolyte	Molality		Conductivity
	m		$ohm^{-1}cm^{-1}$
Propylene carbonate-$LiClO_4$	1.0		6.8×10^{-3}
Propylene carbonate-$AlCl_3$ + LiCl		(2)	5.5×10^{-3}
Propylene carbonate-$Mg(ClO_4)_2$	0.75		5.5×10^{-3}
Propylene carbonate-KPF_6	1.0		4.5×10^{-3}
Propylene carbonate-$MgCl_2$	0.5	(s)	2.4×10^{-3}
Butyrolactone-$MgCl_2$	0.5	(s)	1.3×10^{-3}

(1)   Concentration with respect to each salt

(2)   0.25 m in $AlCl_3$, saturated with LiCl

(s)   Saturated

*   In order of decreasing conductivity

TABLE I.   ELECTROCHEMICAL SYSTEMS SCREENED – CHLORIDE AND PERCHLORATE ELECTROLYTES

Solute \ Solvent	Acetonitrile	Butyrolactone	Dimethylformamide	Propylene carbonate
LiCl			Ag, Cu (0.5, 1.0, 1.5, 2.5 m)** AgCl (1000, 2000 ppm)* Zn, Cd, Mo, In, Fe	
LiClO$_4$	Zn, Cd	Zn, Cd	Cu, Zn, Cd (0.5, 1.0, 1.5, 2.5 m) Mo, In, Fe	CuO, CuCl$_2$ (500, 1000 ppm) Zn, Cd, Mo, In, Fe
LiCl+LiClO$_4$			Zn, Cd	
AlCl$_3$+LiCl	Ag(a), Zn, Zn(a)		Zn, Cd, Mo, Fe	Zn, Zn(a), Cd, Cd(a)
MgCl$_2$		Ag (500 ppm)* Ni (1000 ppm)	Ag, AgCl (1000, 2000 ppm) Zn, Cd, Mo, In, Fe	Ag (500, 1000 ppm) AgCl (1000, 2000 ppm) Zn, Cd
Mg(ClO$_4$)$_2$			Zn, Cd, Mo, In, Fe	Zn, Cd, Mo, In, Fe

(a) LiCl saturated

*   ppm water added to solution

**   varying solute concentration, molality

TABLE III   ELECTROCHEMICAL SYSTEMS SCREENED - FLUORIDE ELECTROLYTES

Solute \ Solvent	Acetonitrile	Butyrolactone	Dimethylformamide	Propylene carbonate
$LiPF_6$			Ag(a), Cu(a), Ni(a), Zn, Cd	Ag(a), Zn, Cd
KPF_6	Cu, CuF_2, Co (500, 1000 ppm)*		AgF_2, CuF_2, Zn (1.0, 2.0, 3.0 m)** Cd, Mo, In, Fe	Cd, Mo, In, Fe
$LiPF_6 + KPF_6$	Ag, Cu, Zn, Cd			
$LiPF_6 + PF_5$			Zn(b), Zn(c)	
$LiBF_4$	Zn, Cd			

(a) $LiPF_6$ prepared in situ, repeat of $LiPF_6$ (Ozark-Mahoning)

(b)   0.1 m PF_5

(c)   0.2 m PF_5

*   ppm water added to solution

**   varying solute concentration, molality

-7-

1. Systems Involving Chloride and Perchlorate Electrolytes

    a. Silver Electrode

        (1) Acetonitrile solution

The cyclic voltammogram for silver metal in $AlCl_3$ solution saturated with LiCl is shown in Figure 1 (CV-2774). This system shows a single anodic peak and a broad complex cathodic peak with very high current densities. The sweep rate dependence indicates the formation of a soluble anodic product (vanishing discharge peak with decreasing sweep rate).

        (2) Butyrolactone solution

The addition of 500 ppm water to butyrolactone-$MgCl_2$ causes voltage overload for the silver electrode, possibly resulting from high peak currents and low conductance of the electrolyte. The cyclic voltammogram for the anhydrous system was presented earlier (Ref. 2, p. 36).

        (3) Dimethylformamide solutions

The cyclic voltammogram for silver in $MgCl_2$ solution containing 2000 ppm water is shown in Figure 2 (CV-2525). This is compared with Figure 3 (CV-2515) representing a control system with no water additive. The most pronounced effect of the water impurity is to increase the peak-to-peak displacement. In addition, the discharge peak current is decreased in the water-containing solution.

Cyclic sweep measurements were made for silver electrodes in dimethyl-formamide-LiCl solutions of 0.5, 1.5, and 2.5 molar concentration. The anodic and cathodic peaks fall in the high to very high current density range, and the sweep rate dependence indicates the formation of insoluble anodic products. Representative curves are shown in Figure 4 (CV-2605) and Figure 5 (CV-2595). Increasing the salt concentration causes a very marked

increase in peak current densities, although the ΔV_p (peak-to-peak displacement) is also increased. Visual observation indicates a yellow discoloration of the solution which decreases as the salt concentration is raised. A brown discharge product forms on the working electrode.

(4) Propylene carbonate solutions

Addition of 500 and 1000 ppm water to systems of silver electrodes in propylene carbonate-$MgCl_2$ showed only minor effects. Small increases in peak current densities, and a decrease in ΔV_p (from 0. 65 to 0. 43 v) were observed on addition of 1000 ppm water.

b. Silver Chloride Electrode

(1) Dimethylformamide solutions

The cyclic voltammogram for AgCl in dimethylformamide-$MgCl_2$ was reported earlier (Ref. 4, p. 30). The addition of 1000 ppm water causes a 25% increase in current densities for both the cathodic and anodic peaks. Addition of 2000 ppm water results in voltage overload. Otherwise, no appreciable difference in the charge-discharge properties from those observed for the anhydrous system was noted. Cyclic voltammetry of AgCl in LiCl solution was reported earlier (Ref. 4, p. 8). During this period, measurements were repeated using solutions containing 1000 and 2000 ppm water. Figures 6 and 7 (CV-2549, CV-2539) show the results obtained with and without water respectively. The addition of 2000 ppm water results in a much higher discharge peak, as well as a very large decrease in ΔV_p. This is not borne out, however, by the earlier measurements made in the absence of added water. In this case, AgCl in dimethylformamide-LiCl gave exceedingly high current densities (in excess of 1. 5 amps/cm^2) for both the charge and discharge reactions). Also, the ΔV_p value was comparable to that for the water-containing solution (Figure 6). It is therefore likely that these discrepancies reflect variations in the chlorination depth of these electrodes rather than the effect of the water

additive. Figure 7 could reasonably be explained by an included IR drop at the working electrode surface.

(2)   Propylene carbonate solutions

The addition of 1000 ppm water to propylene carbonate-$MgCl_2$ causes a significant increase in current densities for both anodic and cathodic peaks in the case of the AgCl electrode. Voltage overload occurs at 2000 ppm water. In addition, the peaks are much sharper than those obtained in solutions without water additive. Unlike the results obtained for dimethyl-formamide-$MgCl_2$, the cyclic voltammograms for the non-treated solutions obtained earlier (Ref. 4, p. 33) and repeated as a control for the water additive screening, are comparable (in peak heights and ΔV_p). In all cases, however, the peak-to-peak displacement is large (about 0.7 v).

c.   Copper Electrode

(1)   Dimethylformamide solutions

During this period, cyclic voltammograms were obtained for copper in dimethylformamide solutions of LiCl and $LiClO_4$ as a function of solute concentration. Poor electrochemical properties are observed at all concentrations of $LiClO_4$ in dimethylformamide. Erratic multiple anodic peaks are observed at low concentrations, along with two broad cathodic peaks having medium low current densities. The sweep rate behavior at all concentrations indicates a decrease in the availability of cathodic reactant at the lower sweep rates (soluble anodic product). A black reaction product forms at the electrode surface. The solutions turn a yellow-green color, with less discoloration at the higher salt concentrations.

As reported earlier (Ref. 3, p. 29), copper in dimethylformamide-LiCl (0.75 m) exhibits multiple anodic peaks and a single cathodic peak. Also the formation of a soluble anodic product is indicated. The most recent data

indicates that changing the solute concentration from 0. 5 to 2. 5 m increases the solubility of the anodic product. In all cases, a black reaction product is observed on the working electrode. Cyclic voltammograms taken for solutions containing 0.5 and 2. 5 m LiCl are shown in Figures 8 and 9 (CV-2594, CV-2579) respectively.

d. Copper Oxide Electrode

(1) Propylene carbonate solutions

The cyclic voltammogram for CuO in propylene carbonate-LiClO$_4$ has been presented earlier (Ref. 2, p. 69). Two anodic peaks and one cathodic peak with high current densities are generally observed. The addition of 500 and 1000 ppm water causes the disappearance of one of the anodic peaks and increases the current density of the remaining anodic peaks as well as the cathodic peak. Voltage sweep curves for the anhydrous system and for that containing 1000 ppm water are shown in Figures 10 and 11 (CV-2550, CV-2557) respectively. The earlier results (Ref. 2, p. 69) showed a much sharper cathodic peak than produced in Figure 10, at double the current density. Also, the initial anodic peak is lower than the second anodic peak.

e. Copper Chloride Electrode

(1) Propylene carbonate solutions

Copper chloride electrodes which exhibited very high anodic and cathodic currents in distilled propylene carbonate-LiClO$_4$, result in voltage overload in solutions containing 500 and 1000 ppm water.

f. Nickel Electrode

(1) Butyrolactone Solution

Previous results with nickel electrodes in butyrolactone-MgCl$_2$ have shown limited anodic and no cathodic activity. The addition of water increases the

anodic activity but fails to improve the cathodic behavior of the nickel electrode in this system.

g. Zinc Electrode

(1) Acetonitrile solutions

The cyclic voltammogram for zinc in $LiClO_4$ solution is shown in Figure 12 (CV-2739). Single anodic and cathodic peaks are observed having very high current densities, with 0.19 v peak-to-peak separation. Sweep rate behavior indicates formation of a soluble cathodic material.

Current overload is obtained in $LiCl + AlCl_3$ solution. Saturation of this solution with LiCl eliminates the current overload condition, and a sweep curve is obtained with two closely spaced anodic peaks of very high current density (1100 ma/cm^2), and a single cathodic peak. Voltage sweeps at 80 and 200 mv/sec result in current overload.

(2) Butyrolactone solution

Zinc in $LiClO_4$ solution shows a single anodic and two cathodic peaks in the medium low current density range. The two cathodic peaks, separated by 0.3 v, suggest a complex discharge process. Sweep rate behavior indicates an insoluble cathode.

(3) Dimethylformamide solutions

The concentration of $LiClO_4$ in dimethylformamide has a pronounced effect on the cyclic voltammograms for zinc electrodes in this electrolyte. Measurements were taken at four concentrations from 0.5 to 2.5 m. Generally, a single cathodic peak and two anodic peaks separated by about 0.8 v are observed as shown in Figure 13 (CV-2668). The peak current density of the first anodic peak falls off from 462 ma/cm^2 to 144 ma/cm^2 as the salt concentration is raised. The current density of the second anodic peak is 36 ma/cm^2

at 2.5 m and has a maximum value of 240 ma/cm^2 at 1.5m. No definite second anodic peak occurs at the lowest concentration range, 0.5 m. Instead, a reverse anodic peak occurs in an erratic region immediately anodic to the first peak. This erratic region extends over an 800 mv range positive to the first peak, and the reverse peak occurs anywhere within this region, varying for each cycle. This is shown in Figure 14 (CV-2675). At higher sweep rates, a third broad anodic peak appears in the region between the two main peaks (Figure 15, CV-2667).

Zinc in LiCl + LiClO$_4$ solution shows multiple anodic peaks and a single sharp cathodic peak in the high current density range. Formation of a soluble cathode material is indicated. These results are similar to those obtained for LiClO$_4$ solution except that higher and sharper peaks occur in the latter.

The cyclic voltammograms for zinc electrodes in Mg(ClO$_4$)$_2$ solutions show curves with poor reproducibility. A single cathodic peak and multiple non-reproducible anodic peaks are observed. A black reaction product forms on the zinc working electrode. Zinc electrodes in LiCl, MgCl$_2$ and AlCl$_3$ + LiCl solutions all cause voltage overload.

(4) Propylene carbonate solutions

The cyclic voltammogram for zinc in LiClO$_4$ solution is shown in Figure 16 (CV-2709). The curve shows relatively sharp peaks in the medium high current density range. The large peak-to-peak separation (ΔV_p = 1.5 v) indicates high activation polarization. Sweep rate behavior predicts soluble cathodic reactants.

The cyclic voltammograms for zinc electrodes in Mg(ClO$_4$)$_2$ solutions show broad peaks with low current densities for both anodic and cathodic processes.

Zinc in $AlCl_3$ + LiCl solution shows a single anodic peak of medium high current density and a broad cathodic peak in the low current density range. Comparison of cathodic peak area with the anodic peak area indicates a low discharge-to-charge efficiency. Saturation of this solution with LiCl has no significant effect on the cyclic voltammogram. Zinc in $MgCl_2$ solution results in voltage overload.

h. Cadmium Electrode

Cadmium in acetonitrile and butyrolactone solutions of $LiClO_4$ results in current overload.

(1) Dimethylformamide solutions

The effect of solute concentration on the cyclic voltammetry of the cadmium electrode has been determined for $LiClO_4$ in dimethylformamide at concentrations ranging from 0.5 to 2.5 m. Very high anodic and cathodic peak current densities are observed at all concentrations. A general trend of increasing anodic and decreasing cathodic peak current densities occurs with increasing salt concentration. However, the number of coulombs/cm^2 expended for both anodic and cathodic processes becomes smaller, and the discharge-to-charge coulombic ratio larger, as the salt concentration is raised from 1.0 m to 2.5 m. Sweep indices show a general increase for the anodic peak and a decrease for the cathodic peak with increasing concentration. The largest current density and discharge capacity for the cathodic peak occurs with the 1.0 m solution indicating optimum cathodic activity in this concentration range. Although the curves generally show a single reproducible charge and discharge peak, an additional erratic and non-reproducible discharge process occurs in some cases at potentials negative to the main cathodic peak. Sweep curves at low and high salt concentrations are shown in Figure 17 (CV-2691) and Figure 18 (CV-2690). Visual observations indicate a black reaction product on the surface of the cadmium electrode and in suspension to some extent at all concentrations.

Cadmium in LiCl solution (Figure 19, CV-2716) shows poor discharge properties, and a cathodic to anodic coulombic ratio less than 0.01. The sweep curve for cadmium in LiCl + LiClO$_4$ solution is shown in Figure 20 (CV-2767). The curve approximates a superimposition of the separate curves for the component salt solutions alone. Although the general shape of the curve is reproducible, an additional sporadic and non-reproducible discharge process occurs at potentials negative to the main reactions. This sporadic peak behavior is similar to that discussed above for cadmium in dimethylformamide-LiClO$_4$ solutions.

Irreproducible peaks with very high current densities are also observed for cadmium in Mg(ClO$_4$)$_2$ for the cathodic reaction. In this case, the reproducibility of the voltage sweep curves is improved as the sweep rate is increased. Sporadic peaks are no longer observed at the 200 mv/sec sweep rate. The sporadic behavior is similar to that observed for LiClO$_4$ solutions, and probably results from non-reproducible changes in surface structure such as in the formation and break-up of non-conducting films. CV curves for cadmium electrodes in AlCl$_3$ + LiCl solution show multiple anodic and cathodic peaks of low current density. A poor charging efficiency is indicated according to the low ratio of cathodic to anodic peak area.

Very low cathodic activity is obtained in MgCl$_2$ solution. Comparison of cathodic to anodic peak heights with sweep rate indicates formation of a soluble cathodic material.

(2) Propylene carbonate solutions

The cyclic voltammogram for cadmium in AlCl$_3$ and LiCl solution is shown in Figure 21 (CV-2785). This system shows two anodic peaks of low current density separated by 0.8 v, and a single sharp cathodic peak of medium low current density. Formation of an insoluble cathodic material is indicated. Saturation of this solution with LiCl reduces both anodic and cathodic activity

to very low current densities. Cadmium in $LiClO_4$ solution results in current overload. The curve in $MgCl_2$ solution shows broad peaks with low activity, probably due to the low solubility of $MgCl_2$ in propylene carbonate.

The CV curve for cadmium in $Mg(ClO_4)_2$ solution is shown in Figure 22 (CV-2826). The curve shows sharp single anodic and cathodic peaks of low current density. The sweep rate dependence of the peak height ratio indicates the formation of an insoluble anodic product.

i.   Molybdenum Electrode

(1)   Dimethylformamide solutions

Molybdenum in chloride and in perchlorate solutions shows low cathodic activity and medium anodic activity. Anodic peaks are broad and no cathodic peaks are observed. The voltage separation between anodic and cathodic activity is usually greater than 1 volt. A cyclic voltammogram for molybdenum in $Mg(ClO_4)_2$ solution is shown in Figure 23 (CV-2856). The absence of a reduction peak in the presence of the broad oxidation peak at all sweep rates illustrates the lack of cathodic activity of this electrode.

(2)   Propylene carbonate solutions

The results for molybdenum in perchlorate solutions are similar to those described for the dimethylformamide solutions. The sweep curves generally show low anodic and very low cathodic activity.

j.   Indium Electrode

These represent the first results reported for indium electrodes.

(1)   Dimethylformamide solutions

Indium in $LiClO_4$ solution shows very high anodic activity and medium cathodic

-16-

activity. The sweep rate dependence of the ratio of the cathodic to anodic peak area indicates the formation of soluble anodic products. Solution discoloration and a dark cloudy suspension are observed. Similar results are obtained for $Mg(ClO_4)_2$ solutions except that peak current densities are lower by a factor of four.

The cyclic voltammogram for indium in LiCl solution shows anodic plateaus of medium high current density and a cathodic peak in the medium low range. Sweep rate dependence suggests soluble anodic products are involved in the electrode process. In $MgCl_2$ solution, indium electrodes show erratic anodic activity of very high current densities, but no cathodic activity.

(2) Propylene carbonate solutions

The cyclic voltammogram for indium in $LiClO_4$ solution is shown in Figure 24 (CV-2927). The curve shows broad peaks in the medium high current density range. The ratio of cathodic to anodic peak areas is 0. 5.

In $Mg(ClO_4)_2$ solutions, two anodic peaks and a single sharp cathodic peak of very high current density are observed. Again, as with $LiClO_4$ solutions, the cathodic peak area is half that of the anodic peak area as shown in Figure 25 (CV-2901). This result may reflect a difference in charge and discharge stoichimetry, i. e., the actual number of electrons per molecule undergoing discharge may be less than required for complete reduction to the metallic state.

k. Iron Electrode

These represent the first results reported for iron electrodes.

(1) Dimethylformamide solutions

The cyclic voltammogram for iron in $LiClO_4$ solution is shown in Figure 26 (CV-2937). No cathodic peak is observed. A sharp anodic peak of high current density occurs on the forward sweep. A repetitive anodic peak is observed on the reverse sweep. Iron in $Mg(ClO_4)_2$ solution yields a voltage sweep curve similar to that described for $LiClO_4$ solution . Complex anodic peaks and lack of cathodic activity has been characteristic of iron systems with chloride and perchlorate electrolytes examined thus far. The highest anodic activity occurs for LiCl solution accompanied by voltage overload. The lowest anodic activity is observed in $MgCl_2$ solution.

(2) Propylene carbonate solutions

The electrochemical behavior of iron in $LiClO_4$ and $Mg(ClO_4)_2$ solutions is similar to that observed in dimethylformamide solutions except that lower current density ranges are involved. Here again no cathodic activity is observed.

2. Systems Involving Fluoride Electrolytes

a. Silver Electrode

(1) Acetonitrile solution

The voltage sweep curve for KPF_6 + $LiPF_6$ solution indicates poor discharge properties. The coulombic ratio is less than 0.1 and the sweep rate behavior indicates formation of a soluble cathodic material. Earlier work with $LiPF_6$ resulted in current overload and dissolution of the electrode. The sweep curve for the mixed salt system is similar to that for silver in the KPF_6 solution alone (Ref. 2, p. 70).

(2) Dimethylformamide solutions

The system silver/DMF-$LiPF_6$, is the only one found thus far which yields

a well defined cathodic peak in the absence of an anodic peak. Formation
of a soluble anodic product is indicated, and visual inspection of the working
electrode revealed that its diameter had been reduced to approximately
half its original size.

(3) Propylene Carbonate solutions

The cyclic voltammogram for silver electrode in $LiPF_6$ solution shows a
very high anodic peak (600 ma/cm^2) and a smaller cathodic peak (140 ma/cm^2).
A comparison of cathodic to anodic peak areas at the slow sweep rate (40 mv/sec)
indicates a poor discharge-to-charge efficiency for this system. Current
overload occurs at higher sweep rates.

b.   Silver Difluoride Electrode

(1)   Dimethylformamide solutions

AgF_2 electrodes in dimethylformamide-KPF_6 solutions at various concen-
trations exhibit erratic behavior and very high currents causing system
oscillation and current overload. No further study of this system was
attempted.

c.   Copper Electrode

(1)   Acetonitrile solutions

The CV curve for copper in KPF_6 + $LiPF_6$ solution, shown in Figure 27
(CV-2751), indicates a well-behaved reversible system with sharp single
anodic and cathodic peaks of very high current density. The ΔV_p is only
70 mv. The sweep indices are 198 and 704 for anodic and cathodic peaks
respectively, and the coulombic ratio is 0.36. Sweep rate behavior
indicates an insoluble cathode. This system is recommended for further
study.

Results on the effect of water addition on Cu in acetonitrile-KPF_6 were inconclusive. Current overload was encountered for both dry solutions and those containing 500 and 1000 ppm water. These results are not in agreement with earlier studies where anodic and cathodic peaks, well within instrumental limitations, were observed for the anhydrous system.

(2) Dimethylformamide solution

The results with copper electrodes in $LiPF_6$ solution indicate very high anodic and cathodic activity accompanied by apparent dissolution of the working electrode, since copper was observed to plate out at the counterelectrode.

d. Copper Fluoride Electrode

(1) Acetonitrile solutions

Results on the effect of water addition on CuF_2 in acetonitrile-KPF_6 were inconclusive. Current overload was encountered for both dry solutions and those containing 500 and 1000 ppm water. These results are not in agreement with earlier studies where anodic and cathodic peaks, well within instrumental limitations, were observed for the anhydrous system.

(2) Dimethylformamide solutions

The effect of concentration of KPF_6 in dimethylformamide was determined for copper fluoride in 1.0, 2.0, and 3.0 m solutions. Changing the concentration had no appreciable effect on the cyclic voltammograms of this system. This is in agreement with earlier data obtained at 0.75 m (Ref. 3, p. 56). Medium low to medium high anodic peaks were obtained with vanishing cathodic peaks at the lower sweep rates indicating formation of a soluble anodic product.

e. Nickel Electrode

(1) Dimethylformamide solution

The cyclic voltammogram for nickel in $LiPF_6$ solution shows high anodic but no cathodic activity, similar to previous results with this metal in fluoride electrolytes.

f. Cobalt Electrode

(1) Acetonitrile solution

Cobalt in KPF_6 solution shows anodic but no cathodic activity. Addition of 500 ppm and 1000 ppm water to this system increases the anodic activity but fails to show any improvement in cathodic behavior.

g. Zinc Electrode

(1) Acetonitrile solutions

Zinc in $LiBF_4$ solution results in anodic current overload, and causes a darkening of the solution. Anodic current overload is also obtained in $KPF_6 + LiPF_6$ solution.

(2) Dimethylformamide solutions

The effect of KPF_6 concentration in dimethylformamide was determined for zinc in 1.0, 2.0, and 3.0 m solutions. The results are shown in Figures 28 and 29 (CV-2657, CV-2645) for the 1.0 and 3.0 m solutions respectively. As indicated, a single sharp anodic and cathodic peak is obtained in each case. The cathodic peak current density shows a maximum value for the 2.0 m solution, whereas the anodic peak current density generally decreases with increasing concentration. Optimum overall performance occurs at this concentration, where the highest values for the cathodic peak current density, coulombic ration, and sweep index are observed. Lowest values for these

sweep parameters occur for the 3.0 m solution, possibly due to the increased viscosity. In all cases, a black reaction product forms on the zinc electrode.

The cyclic voltammogram for zinc in $LiPF_6$ solution is shown in Figure 30 (CV-2733). The CV curve shows single sharp anodic and cathodic peaks with very high current densities and low peak-to-peak separation. Sweep-rate behavior indicates formation of an insoluble cathode. Addition of 0.1 m excess PF_5 causes no significant change in the sweep curve, although the formation of bubbles on the zinc surface was observed. Addition of 0.2 m excess PF_5 increases the gassing at the zinc surface and broadens the anodic peak in the CV curve. Apparently, excess PF_5 is detrimental to this system.

(3) Propylene carbonate solution

Zinc in propylene carbonate-$LiPF_6$ shows a broad, low current density anodic and cathodic peak, but with erratic behavior in the form of superimposed irreproducible low current spikes.

h. Cadmium Electrode

(1) Acetonitrile solutions

Cadmium in KPF_6 + $LiPF_6$ solution, as well as in $LiBF_4$ solution, results in anodic current overload of the instrumentation. Instrument oscillation prevented observation of the cathode sweep.

(2) Dimethylformamide solutions

The CV curve for cadmium in KPF_6 solution is not reproducible. Very high single anodic and cathodic peaks are obtained with peak-to-peak separation of 100-200 mv. This system is recommended for further study.

Cadmium in $LiPF_6$ solution results in both anodic and cathodic current

overload with solution discoloration.

(3) Propylene carbonate solutions

Cadmium in KPF_6 solution shows a broad anodic and a sharp cathodic peak with very high current density. Reproducibility is poor, and current overload occurs at the higher sweep rates so that an indication of cathode solubility cannot be obtained. Cadmium in propylene carbonate-$LiPF_6$ causes current overload.

i. Molybdenum Electrode

(1) Dimethylformamide solution

Molybdenum electrodes in KPF_6 solution show low anodic and no cathodic activity.

(2) Propylene carbonate solution

The result for molybdenum in KPF_6 solution are similar to those obtained in dimethylformamide, namely, low anodic and very low cathodic activity.

j. Indium Electrode

(1) Dimethylformamide solution

The cyclic voltammogram for indium in KPF_6 solution shows two broad anodic peaks of very high current density, repetitive anodic peaks on the reverse sweep, and a medium low cathodic peak. A dark brown discoloration of the solution accompanies the cycling process. The voltage sweep curves thus indicate complex anodic reactions yielding products of limited utility on discharge.

(2) Propylene carbonate solution

Indium in KPF_6 solution results in voltage overload caused by very high

current densities for both anodic and cathodic sweeps. A metal, presumably indium, is observed to plate out at the counterelectrode indicating that the high reactivity of indium electrodes in this electrolyte results from high solubility of electrode reaction products.

k. Iron Electrode

(1) Dimethylformamide solution

The cyclic voltammogram for iron in KPF_6 solution shows a low anodic and very low cathodic activity. No peaks are observed for this system.

(2) Propylene carbonate solutions

The cyclic voltammogram for iron electrode in KPF_6 solution is shown in Figure 31 (CV-2893). A single anodic peak of medium low current density appears at the extreme anodic voltage range and a low current density cathodic current occurs at the cathodic voltage limit.

Electrode - Ag
Electrolyte - Acetonitrile-LiCl + AlCl₃
Sweep rate - 40 mv/sec
Temp. 30°C
Zero ref. -0.50 v/Pt
CV-2774

VOLTS POLARIZATION

Figure 1

Figure 2

Electrode - Ag
Electrolyte - Dimethylformamide-$MgCl_2$ + 2000 ppm H_2O
Sweep rate - 40 mv/sec
Temp. 30° C
Zero ref. -0.06 v/Pt
CV - 2525

VOLTS POLARIZATION

CHARGE

ma/cm^2

DISCHARGE

Figure 3

The figure shows a cyclic voltammetry plot with the following parameters:

Electrode - Ag
Electrolyte - Dimethylformamide-$MgCl_2$
Sweep rate - 40 mv/sec
Temp. 30° C
Zero ref. -0.05 v/Pt
CV - 2515

Y-axis: ma/cm^2 with CHARGE (160.0, 0.0) and DISCHARGE (-160.0, -320.0, -480.0, -640.0)

X-axis: VOLTS POLARIZATION (-1.0, -0.8, -0.6, -0.4, -0.2, 0, 0.2, 0.4, 0.6, 0.8, 1.0)

Figure 4

Electrode - Ag
Electrolyte - Dimethylformamide-LiCl (0.5 m)
Sweep rate - 40 mv/sec
Temp. 30°C
Zero ref. -0.14 v/Pt
CV - 2605

VOLTS POLARIZATION

CHARGE

DISCHARGE

ma/cm²

Electrode - Ag
Electrolyte - Dimethylformamide-LiCl (2.5 m)
Sweep rate - 40 mv/sec
Temp. 30°C
Zero ref. +0.34 v/Pt
CV - 2595

Figure 5

Figure 6

Electrode - AgCl
Electrolyte - Dimethylformamide-LiCl + 2000 ppm H_2O
Sweep rate - 40 mv/sec
Temp. 30° C
Zero ref. -0.06 v/Pt
CV - 2549

VOLTS POLARIZATION

CHARGE

DISCHARGE

ma/cm^2

Figure 7

Electrode - AgCl
Electrolyte - Dimethylformamide-LiCl
Sweep rate - 40 mv/sec
Temp. 30°C
Zero ref. -0.06 v/Pt
CV - 2539

VOLTS POLARIZATION

CHARGE

DISCHARGE

ma/cm^2

Figure 8

CHARGE · DISCHARGE

ma/cm²

160.2 · 106.8 · 53.4 · 0.0 · -53.4 · -106.8 · -160.2

VOLTS POLARIZATION

Electrode - Cu
Electrolyte - Dimethylformamide-LiCl (0.5 m)
Sweep rate - 40 mv/sec
Temp. 30°C
Zero ref. -0.30 v/Pt
CV - 2594

Electrode   -   Cu
Electrolyte -   Dimethylformamide-LiCl (2.5m)
Sweep rate   -   40 mv/sec
Temp.   30°C
Zero ref.   -0.04 v/Pt
CV - 2579

CHARGE - ma/cm²

VOLTS POLARIZATION

Figure 9

Figure 10

Electrode - CuO
Electrolyte - Propylene carbonate-LiClO$_4$
Sweep rate - 40 mv/sec
Temp. 30°C
Zero ref. 0.00 v/Pt
CV - 2550

CHARGE

DISCHARGE

ma/cm^2

VOLTS POLARIZATION

-34-

Electrode - CuO
Electrolyte - Propylene carbonate-LiClO$_4$ + 1000 ppm H$_2$O
Sweep rate - 40 mv/sec
Temp. 30°C
Zero ref. 0.00 v/Pt
CV - 2557

CHARGE

DISCHARGE

ma/cm^2

VOLTS POLARIZATION

Figure 11

-35-

Figure 12

Electrode - Zn
Electrolyte - Acetonitrile-LiClO₄
Sweep rate - 40 mv/sec
Temp. 30°C
Zero ref. -0.60 v/Pt
CV-2739

CHARGE

DISCHARGE

ma/cm²

VOLTS POLARIZATION

Figure 13

Electrode - Zn
Electrolyte - Dimethylformamide-LiClO$_4$(1.5m)
Sweep rate - 40 mv/sec
Temp. 30°C
Zero ref. -0.38 v/Pt
CV - 2668

VOLTS POLARIZATION

CHARGE

DISCHARGE

ma/cm^2

Figure 14

Electrode - Zn
Electrolyte - Dimethylformamide - LiClO$_4$ (0.5m)

Sweep rate - 40 mv/sec
Temp. 30°C
Zero ref. -0.38 v/Pt
CV - 2675

Erratic Region

VOLTS POLARIZATION

CHARGE

DISCHARGE

ma/cm^2

Figure 15

Electrode - Zn
Electrolyte - Dimethylformamide-LiClO$_4$ (1.5 m)
Sweep rate - 80 mv/sec
Temp. 30° C
Zero ref. -0.38 v/Pt
CV - 2667

CHARGE

DISCHARGE

ma/cm^2

VOLTS POLARIZATION

Figure 16

Electrode - Zn
Electrolyte - Propylene carbonate-LiClO$_4$
Sweep rate - 40 mv/sec
Temp.   30°C
Zero ref. -0. 30 v/Pt
CV-2709

VOLTS POLARIZATION

CHARGE

DISCHARGE

ma/cm^2

128. 0

96. 0

64. 0

32. 0

0. 0

-32. 0

-64. 0

1. 0   0. 8   0. 6   0. 4   0. 2   0   -0. 2   -0. 4   -0. 6   -0. 8   -1. 0

-40-

Electrode - Cd
Electrolyte - Dimethylformamide-LiClO$_4$ (0.5 m)
Sweep rate - 40 mv/sec
Temp. 30° C
Zero ref. -0.60 v/Pt
CV - 2691

*Sporadic peak

VOLTS POLARIZATION

Figure 17

Figure 18

Electrode - Cd
Electrolyte - Dimethylformamide-LiClO$_4$ (1.5 m)

Sweep rate - 40 mv/sec
Temp. 30° C
Zero ref. 0.0 v/Pt
CV - 2690

VOLTS POLARIZATION

CHARGE

DISCHARGE

ma/cm^2

Electrode - Cd
Electrolyte - Dimethylformamide-LiCl
Sweep rate - 40 mv/sec
Temp. 30°C
Zero ref. -0.48 v/Pt
CV-2716

VOLTS POLARIZATION

Figure 19

Electrode - Cd
Electrolyte - Dimethylformamide - LiClO$_4$ + LiCl
Sweep rate - 40 mv/sec
Temp. 30° C
Zero ref. -0.23 v/Pt
CV-2767

VOLTS POLARIZATION

Figure 20

-44-

Electrode - Cd

Electrolyte - Propylene carbonate-LiCl + AlCl$_3$

Sweep rate - 40 mv/sec

Temp. 30°C

Zero ref. -0.52 v/Pt

CV-2785

VOLTS POLARIZATION

Figure 21

CHARGE

DISCHARGE

ma/cm^2

Figure 22

Electrode — Cd
Electrolyte — Propylene carbonate—Mg(ClO$_4$)$_2$
Sweep rate — 40 mv/sec
Temp. — 30°C
Zero ref. —0.20 v/Pt
CV — 2826

VOLTS POLARIZATION

CHARGE

DISCHARGE

ma/cm^2

Electrode   - Mo
Electrolyte - Dimethylformamide-Mg(ClO$_4$)$_2$
Sweep rate - 40 mv/sec
Temp.   - 30° C
Zero ref.   +0.60v/Pt
CV - 2856

VOLTS POLARIZATION

Figure 23

CHARGE

DISCHARGE

ma/cm^2

96.0   76.8   57.6   38.4   19.2   0.0   -19.2

-47-

Figure 24

Electrode - In
Electrolyte - Propylene carbonate LiClO$_4$
Sweep rate - 40 mv/sec
Temp. - 30° C
Zero ref. -0.20v/Pt
CV - 2901

VOLTS POLARIZATION

CHARGE

DISCHARGE

ma/cm^2

684.0   456.0   228.0   0.0   -228.0   -456.0

-48-

Figure 25

Electrode   -   In
Electrolyte -   Propylene carbonate - LiClO$_4$
Sweep rate   -   40 mv/sec
Temp.   -   30° C
Zero ref.   0.00v/Pt
CV - 2927

VOLTS POLARIZATION

CHARGE   DISCHARGE

ma/cm^2

Electrode — Fe
Electrolyte — Dimethylformamide-LiClO$_4$
Sweep rate — 40 mv/sec
Temp. — 30°C
Zero ref. +0.60v/Pt
CV — 2937

CHARGE

ma/cm^2

DISCHARGE

VOLTS POLARIZATION

Figure 26

Electrode - Cu

Electrolyte - Acetonitrile-KPF$_6$ + LiPF$_6$

Sweep rate - 40 mv/sec

Temp. 30°C

Zero ref. -1.02 v/Pt

CV-2751

VOLTS POLARIZATION

Figure 27

Electrode - Zn
Electrolyte - Dimethylformamide-KPF$_6$ (1.0 m)
Sweep rate - 40 mv/sec
Temp. 30°C
Zero ref. -0.68 v/Pt
CV - 2657

VOLTS POLARIZATION

Figure 28

CHARGE   ma/cm^2 DISCHARGE

Figure 29

Electrode - Zn
Electrolyte - Dimethylformamide-KPF$_6$ (3.0 m)
Sweep rate - 40 mv/sec
Temp. 30°C
Zero ref. -0.98 v/Pt
CV - 2645

CHARGE   ma/cm^2 DISCHARGE

VOLTS POLARIZATION

Electrode - Zn
Electrolyte - Dimethylformamide-LiPF$_6$
Sweep rate - 40 mv/sec
Temp. 30° C
Zero ref. -1.0 v/Pt
CV-2733

VOLTS POLARIZATION

Figure 30

Electrode   - Fe
Electrolyte - Propylene carbonate - KPF_6
Sweep rate   - 40 mv/sec
Temp.   - 30° C
Zero ref.   0.00v/Pt
CV - 2893

Figure 31

-55-

B.   TABLES OF CYCLIC VOLTAMMETRIC DATA

Included in this section are tables listing parameters derived from the cyclic voltammograms. These parameters are as follows:

1.   Sweep index - This is a relative figure of merit taking into account peak heights, sweep rate, and discharge capacity. This parameter is described in more detail in an earlier report (Ref. 1, p. 80).

2.   Peak current density range - Relative magnitude of peak currents classified according to page 2.

3. ΔV_p - Peak-to-peak displacement in volts of charge and discharge reactions giving a measure of overall electrode reversibility, or in more practical terms, a measure of suitability of the electrochemical system for second battery application.

4.   Coulombic ratio - Ratio of cathodic to anodic peak area. Values significantly in excess of unity for the pre-formed electrodes (chlorinated and fluorinated metals) are indicative of the contribution of the original cathodic material to the discharge reaction independent of the material formed by the preceding charge sweep.

5.   Discharge capacity - Measure of discharge utilization per unit area of electrode surface, when compared with the coulombic ratio except for values of the latter greater than unity.

Also included are tables listing the systems causing voltage and current overload of the instrumentation preventing recordable 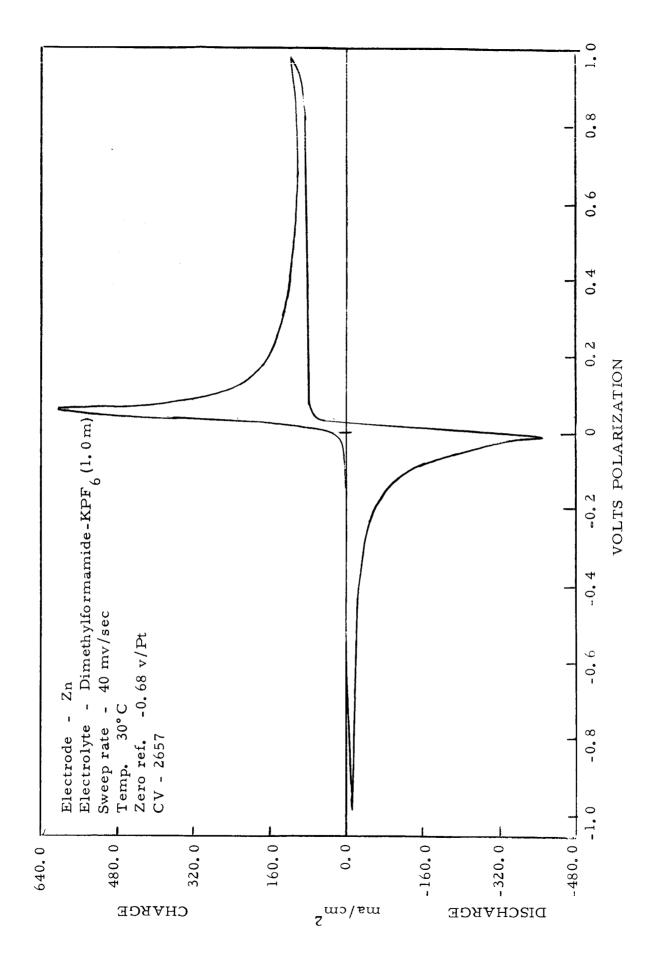voltammograms as well as those systems failing to exhibit either anodic or cathodic peaks. In cases of solutions having varying molality, the concentrations are included with the designated system. The concentration of all solutions are listed in Table I.

TABLE IV

SYSTEMS CAUSING VOLTAGE OVERLOAD
OF INSTRUMENTATION
CHLORIDE AND PERCHLORATE ELECTROLYTES

System	CV	Max. Anod. C.D. ma/cm^2	Max. Cath. C.D. ma/cm^2
$Ag/BL-MgCl_2$ (a)	2527	272	280
$AgCl/DMF-MgCl_2$ (c)	2535	nr*	nr
$AgCl/PC-MgCl_2$ (c)	2538	200	300
$CuCl_2/PC-LiClO_4$ (b)	2560	400	800
$CuCl_2/PC-LiClO_4$ (a)	2559	1200	1600
$Ni/BL-MgCl_2$ (b)	2532	nr	nil
$Zn/DMF-AlCl_3+LiCl$	2847	1600	nr
$Zn/DMF-MgCl_2$	2803	1600	nr
$Zn/PC-MgCl_2$	2809	nr	nr
$Cd/PC-LiClO_4$	2710	320	2140
$Fe/DMF-LiCl$ (0.5 m)	2902	1600	nr

(a) Containing 500 ppm water

(b) Containing 1000 ppm water

(c) Containing 2000 ppm water

*   Not recordable due to instrument oscillation resulting from amplifier mismatch with varying cell impedance.

BL   -   Butyrolactone
DMF -   Dimethylformamide
PC   -   Propylene carbonate

TABLE V

SYSTEMS CAUSING VOLTAGE OVERLOAD
OF INSTRUMENTATION
FLUORIDE ELECTROLYTES

System	CV	Max. Anod. C.D. ma/cm^2	Max. Cath. C.D. ma/cm^2
AgF_2/DMF-KPF_6 (3.0 m)	2621	nr*	nr
AgF_2/DMF-KPF_6 (1.5 m)	2622	nr	nr
In/PC-KPF_6	2899	1600	800

*   - Not recordable due to instrument oscillation

DMF - Dimethylformamide

PC   - Propylene carbonate

TABLE VI

SYSTEMS CAUSING CURRENT OVERLOAD**
OF INSTRUMENTATION
CHLORIDE AND PERCHLORATE ELECTROLYTES

System	CV	Max. Anod. C. D. ma/cm^2	Max. Cath. C. D. ma/cm^2
Cu/DMF-LiClO$_4$ (0.5 m)	2640	nr*	nr
Zn/AN-AlCl$_3$+LiCl	2768	ov**	ov
Zn/DMF-LiCl (1.0 m)	2711	ov	ov
Cd/AN-LiClO$_4$	2740	ov	nr
Cd/BL-LiClO$_4$	2761	ov	ov

*   -   Not recordable due to instrument oscillation
**   -   Maximum current greater than 4.8 amp/cm^2

AN   -   Acetonitrile
BL   -   Butyrolactone
DMF   -   Dimethylformamide

TABLE VII

SYSTEMS CAUSING CURRENT OVERLOAD*
OF INSTRUMENTATION
FLUORIDE ELECTROLYTES

System	CV	Max. Anod. C. D. ma/cm^2	Max. Cath. C. D. ma/cm^2
$Cu/AN-KPF_6$ (b)	2571	ov*	ov
$Cu/AN-KPF_6$ (a)	2570	ov	ov
$CuF_2/AN-KPF_6$ (b)	2574	ov	ov
$CuF_2/AN-KPF_6$ (a)	2573	ov	ov
$Co/AN-KPF_6$ (b)	2568	ov	nr**
$Zn/AN-LiBF_4$	2787	ov	nr
$Zn/AN-KPF_6+LiPF_6$	2754	ov	nr
$Cd/AN-LiBF_4$	2786	ov	nr
$Cd/AN-KPF_6+LiPF_6$	2755	ov	nr
$Cd/DMF-LiPF_6$	2734	ov	ov
$Cd/PC-LiPF_6$	2702	nr	nr

(a) Containing 500 ppm water
(b) Containing 1000 ppm water

*   -   Maximum current greater than 4.8 amp/cm^2
**   -   Not recordable due to instrument oscillation

AN   -   Acetonitrile
DMF   -   Dimethylformamide
PC   -   Propylene carbonate

TABLE VIII

PEAK CURRENT DENSITY RANGE
CHLORIDE AND PERCHLORATE ELECTROLYTES

System	CV	Anodic	Cathodic
Ag/AN-AlCl$_3$+LiCl*	2774	very high	very high
Ag/DMF-LiCl (2.5 m)	2595	very high	very high
Ag/DMF-LiCl (1.5 m)	2596	very high	very high
Ag/DMF-LiCl (1.0 m)	2600	very high	very high
Ag/DMF-LiCl (0.5 m)	2605	high	very high
Ag/DMF-MgCl$_2$ (c)	2525	medium low	high
Ag/DMF-MgCl$_2$ (b)	2520	high	very high
Ag/PC-MgCl$_2$ (b)	2530	high	high
Ag/PC-MgCl$_2$ (a)	2529	medium low	medium low
AgCl/DMF-LiCl (0.75 m) (c)	2549	high	very high
AgCl/DMF-LiCl (0.75 m) (b)	2544	very high	very high
AgCl/DMF-MgCl$_2$ (b)	2534	high	very high
AgCl/PC-MgCl$_2$ (b)	2537	high	high
Cu/DMF-LiCl (1.5 m)	2584	high	medium low
Cu/DMF-LiCl (1.0 m)	2589	high	high
Cu/DMF-LiCl (0.5 m)	2594	high	high
Cu/DMF-LiClO$_4$ (2.5 m)	2627	high	high

*	-	LiCl saturated
AN	-	Acetonitrile
BL	-	Butyrolactone
DMF	-	Dimethylformamide
PC	-	Propylene carbonate

(a) Containing 500 ppm water
(b) Containing 1000 ppm water
(c) Containing 2000 ppm water

TABLE VIII (Cont'd.)

System	CV	Anodic	Cathodic
$Cu/DMF-LiClO_4$ (1.5 m)	2632	high	low
$Cu/DMF-LiClO_4$ (1.0 m)	2638	high	medium high
$CuO/PC-LiClO_4$ (b)	2557	very high	very high
$CuO/PC-LiClO_4$ (a)	2555	high	very high
$Zn/AN-AlCl_3+LiCl*$	2769	very high	high
$Zn/AN-LiClO_4$	2739	very high	very high
$Zn/BL-LiClO_4$	2760	medium low	medium low
$Zn/DMF-LiClO_4$ (2.5 m)	2663	high	medium low
$Zn/DMF-LiClO_4$ (1.5 m)	2668	high	very high
$Zn/DMF-LiClO_4$ (1.0 m)	2680	very high	high
$Zn/DMF-LiClO_4$ (0.5 m)	2675	very high	very high
$Zn/DMF-LiClO_4+LiCl$	2766	high	high
$Zn/DMF-Mg(ClO_4)_2$	2831	very high	very high
$Zn/PC-AlCl_3+LiCl$	2780	medium high	medium low
$Zn/PC-AlCl_3+LiCl*$	2792	medium high	medium low
$Zn/PC-LiClO_4$	2709	high	medium high
$Zn/PC-Mg(ClO_4)_2$	2821	low	low
$Cd/DMF-LiCl$ (1.0 m)	2716	very high	high
$Cd/DMF-AlCl_3+LiCl$	2842	medium high	low
$Cd/DMF-LiClO_4$ (2.5 m)	2688	very high	very high

*	-	LiCl saturated		
AN	-	Acetonitrile	(a)	Containing 500 ppm water
BL	-	Butyrolactone	(b)	Containing 1000 ppm water
DMF	-	Dimethylformamide		
PC	-	Propylene carbonate		

TABLE VIII (Cont'd.)

System	CV	Anodic	Cathodic
$Cd/DMF-LiClO_4$ (1. 5 m)	2690	very high	very high
$Cd/DMF-LiClO_4$ (1. 0 m)	2683	very high	very high
$Cd/DMF-LiClO_4$ (0. 5 m)	2691	very high	very high
$Cd/DMF-LiClO_4+LiCl$	2767	very high	very high
$Cd/DMF-MgCl_2$	2802	medium low	very low
$Cd/DMF-Mg(ClO_4)_2$	2836	high	very high
$Cd/PC-AlCl_3+LiCl$	2785	low	low
$Cd/PC-AlCl_3+LiCl*$	2797	very low	very low
$Cd/PC-MgCl_2$	2808	low	very low
$Cd/PC-Mg(ClO_4)_2$	2826	low	low
$In/DMF-LiCl$ (0. 5 m)	2912	high	medium low
$In/DMF-LiClO_4$ (1. 0 m)	2942	very high	medium low
$In/DMF-Mg(ClO_4)_2$	2888	high	medium high
$In/PC-LiClO_4$	2927	medium high	medium high
$In/PC-Mg(ClO_4)_2$	2901	very high	very high

* - LiCl saturated

AN - Acetonitrile
DMF - Dimethylformamide
PC - Propylene carbonate

TABLE IX

PEAK CURRENT DENSITY RANGE
FLUORIDE ELECTROLYTES

System	CV	Anodic	Cathodic
$Ag/AN-LiPF_6+KPF_6$	2752	very high	high
$Ag/PC-LiPF_6$	2704	very high	high
$Cu/AN-LiPF_6+KPF_6$	2751	very high	very high
$Cu/DMF-LiPF_6$	2718	very high	very high
$Cu/PC-LiPF_6$	2696	high	high
$CuF_2/DMF-KPF_6$ (3.0 m)	2610	low	medium high
$Zn/DMF-LiPF_6$	2733	very high	very high
$Zn/DMF-LiPF_6+PF_5$ (a)	2744	very high	very high
$Zn/DMF-LiPF_6+PF_5$ (b)	2745	high	high
$Zn/DMF-KPF_6$ (3.0 m)	2645	high	high
$Zn/DMF-KPF_6$ (2.0 m)	2651	high	very high
$Zn/DMF-KPF_6$ (1.0 m)	2657	very high	very high
$Zn/PC-LiPF_6$	2703	low	low
$Cd/DMF-KPF_6$ (0.75 m)	2814	very high	very high
$Cd/PC-KPF_6$	2816	high	very high
$In/DMF-KPF_6$ (0.75 m)	2953	very high	medium low

(a)   -   0.1 m PF_5

(b)   -   0.2 m PF_5

AN - Acetonitrile
DMF - Dimethylformamide
PC - Propylene carbonate

TABLE X

SWEEP INDEX*

System	CV	Anodic $\text{ohm}^{-1}\text{cm}^{-2}$	Cathodic $\text{ohm}^{-1}\text{cm}^{-2}$
Ag/DMF-LiCl (2.5 m)	2595	663.0	1210.0
Ag/DMF-LiCl (1.5 m)	2596	218.0	962.0
Ag/DMF-LiCl (1.0 m)	2600	320.0	892.0
Ag/DMF-LiCl (0.5 m)	2605	27.3	397.0
Ag/DMF-MgCl$_2$ (c)	2525	6.4	107.0
Ag/DMF-MgCl$_2$ (b)	2520	332.0	467.0
Ag/PC-MgCl$_2$ (b)	2530	147.0	42.0
Ag/PC-MgCl$_2$ (a)	2529	9.8	4.6
AgCl/DMF-LiCl (0.75 m) (c)	2549	37.8	992.0
AgCl/DMF-LiCl (0.75 m) (b)	2544	218.0	1898.0
AgCl/DMF-MgCl$_2$ (b)	2534	34.0	676.0
AgCl/PC-MgCl$_2$ (b)	2537	111.0	250.0
Cu/AN-LiPF$_6$+KPF$_6$	2751	198.0	704.0
Cu/DMF-LiCl (1.0 m)	2589	-	198.0
Cu/DMF-LiCl (0.5 m)	2594	-	112.0
Cu/PC-LiPF$_6$	2696	45.0	120.0
CuO/PC-LiClO$_4$ (a)	2555	62.7	537.0
Zn/AN-LiClO$_4$	2739	160.0	65.8

(a)	Containing 500 ppm water	AN -	Acetonitrile
(b)	Containing 1000 ppm water	BL -	Butyrolactone
(c)	Containing 2000 ppm water	DMF -	Dimethylformamide
		PC -	Propylene carbonate

$$*\frac{(\text{peak c.d.})^2 \times 100}{\text{sweep rate} \times \text{coul/cm}^2}$$

TABLE X (Cont'd.)

SWEEP INDEX*

System	CV	Anodic $ohm^{-1}cm^{-2}$	Cathodic $ohm^{-1}cm^{-2}$
$Zn/DMF-LiClO_4$ (2.5 m)	2663	72.5	25.0
$Zn/DMF-LiClO_4$ (1.5 m)	2668	-	391.0
$Zn/DMF-LiClO_4$ (1.0 m)	2680	-	310.0
$Zn/DMF-LiClO_4$ (0.5 m)	2675	195.0	563.0
$Zn/DMF-LiPF_6$	2733	66.8	150.0
$Zn/DMF-LiPF_6+PF_5$ (a)	2744	144.0	263.0
$Zn/DMF-KPF_6$ (3.0 m)	2645	192.0	92.7
$Zn/DMF-KPF_6$ (2.0 m)	2651	625.0	335.0
$Zn/DMF-KPF_6$ (1.0 m)	2657	123.0	283.0
$Cd/DMF-LiClO_4$ (2.5 m)	2688	667.00	835.0
$Cd/DMF-LiClO_4$ (1.5 m)	2690	377.0	1267.0
$Cd/DMF-LiClO_4$ (1.0 m)	2683	53.2	1820.0
$Cd/DMF-LiClO_4$ (0.5 m)	2691	87.2	2260.0
$Cd/DMF-KPF_6$ (0.75 m)	2814	41.2	1260.0
$Cd/PC-AlCl_3+LiCl$	2785	-	15.9
$Cd/PC-KPF_6$	2816	-	782.0
$In/PC-LiClO_4$	2927	9.9	6.7
$In/PC-Mg(ClO_4)_2$	2901	-	507.0

(a)   -   0.1 m PF_5

AN - Acetonitrile
BL - Butyrolactone
DMF - Dimethylformamide
PC - Propylene carbonate

$$*\frac{(peak\ c.d.)^2 \times 100}{sweep\ rate \times coul/cm^2}$$

TABLE XI

ΔV_p, COULOMBIC RATIO, AND DISCHARGE CAPACITY

System	CV	ΔV_p *	Coul. ** Ratio	Disch. Capac. $coul/cm^2$
Ag/DMF-LiCl (2.5 m)	2595	0.35	0.73	6.40
Ag/DMF-LiCl (1.5 m)	2596	0.35	0.54	3.36
Ag/DMF-LiCl (1.0 m)	2600	0.30	0.52	3.72
Ag/DMF-LiCl(0.5 m)	2605	0.24	0.51	1.57
Ag/DMF-MgCl$_2$ (c)	2525	0.36	0.96	0.34
Ag/DMF-MgCl$_2$ (b)	2520	0.21	0.82	1.42
Ag/PC-MgCl$_2$ (b)	2530	0.43	1.34	1.14
Ag/PC-MgCl$_2$ (a)	2529	0.50	0.41	0.31
Ag/PC-LiPF$_6$	2704	0.07	-	-
AgCl/DMF-LiCl (0.75 m) (c)	2549	0.14	0.58	2.03
AgCl/DMF-LiCl (0.75 m) (b)	2544	0.23	0.63	4.33
AgCl/DMF-MgCl$_2$ (b)	2534	0.49	0.63	1.44
AgCl/PC-MgCl$_2$ (b)	2537	0.69	0.58	0.41
Cu/AN-LiPF$_6$+KPF$_6$	2751	0.06	0.36	0.55
Cu/DMF-LiCl (1.0 m)	2589	0.17	-	0.34
Cu/DMF-LiCl (0.5 m)	2594	0.33	-	0.41
Cu/DMF-LiClO$_4$ (2.5 m)	2627	0.04	-	-
Cu/DMF-LiPF$_6$	2718	0.10	-	-

*   -   Voltage separating anodic to cathodic peaks

**   -   Ratio of cathodic to anodic peak areas

AN	-	Acetonitrile	(a)	Containing 500 ppm water
BL	-	Butyrolactone	(b)	Containing 1000 ppm water
DMF	-	Dimethylformamide	(c)	Containing 2000 ppm water
PC	-	Propylene carbonate		

TABLE XI (Cont'd.)

System	CV	ΔV_p *	Coul. ** Ratio	Disch. Capac. coul/cm^2
$Cu/PC-LiPF_6$	2696	0.30	0.72	1.10
$CuO/PC-LiClO_4$ (b)	2557	0.33	-	-
$CuO/PC-LiClO_4$ (a)	2555	0.39	1.49	2.98
$CuF_2/DMF-KPF_6$ (3.0 m)	2610	0.18	-	-
$Zn/AN-LiClO_4$	2739	0.19	1.10	5.62
$Zn/DMF-LiClO_4$ (2.5 m)	2663	0.07	0.71	0.51
$Zn/DMF-LiClO_4$ (1.5 m)	2668	0.01	-	0.73
$Zn/DMF-LiClO_4$ (1.0 m)	2680	0.06	-	0.51
$Zn/DMF-LiClO_4$ (0.5 m)	2675	0.09	0.36	0.97
$Zn/DMF-LiPF_6$	2733	0.06	0.46	2.4
$Zn/DMF-LiPF_6+PF_5$ (c)	2744	0.08	0.44	2.48
$Zn/DMF-LiPF_6+PF_5$ (d)	2745	0.21	-	-
$Zn/DMF-KPF_6$ (3.0 m)	2645	0.06	0.47	0.40
$Zn/DMF-KPF_6$ (2.0 m)	2651	0.09	0.72	0.54
$Zn/DMF-KPF_6$ (1.0 m)	2657	0.08	0.28	1.71
$Zn/PC-LiClO_4$	2709	1.50	-	-
$Cd/DMF-LiClO_4$ (2.5 m)	2688	-	0.86	1.62

(a)	Containing 500 ppm water	(c)	0.1 m PF_5
(b)	Containing 1000 ppm water	(d)	0.2 m PF_5

* — Voltage separating anodic to cathodic peaks
** — Ratio of cathodic to anodic peak areas

AN — Acetonitrile
BL — Butyrolactone
DMF — Dimethylformamide
PC — Propylene carbonate

TABLE XI (Cont'd.)

System	CV	ΔV_p *	Coul. ** Ratio	Disch. Capac. $coul/cm^2$
Cd/DMF-LiClO$_4$ (1.5 m)	2690	0.08	0.50	2.01
Cd/DMF-LiClO$_4$ (1.0 m)	2683	0.05	0.57	3.29
Cd/DMF-LiClO$_4$ (0.5 m)	2691	-	0.29	1.95
Cd/DMF-KPF$_6$ (0.75 m)	2814	0.17	0.19	2.07
Cd/PC-AlCl$_3$+LiCl	2785	-	-	0.11
Cd/PC-KPF$_6$	2816	-	-	2.92
In/DMF-Mg(ClO$_4$)$_2$	2888	0.35	-	-
In/PC-LiClO$_4$	2927	1.00	0.51	0.83
In/PC-Mg(ClO$_4$)$_2$	2901	-	0.54	1.54

*   -   Voltage separating anodic to cathodic peaks

** -   Ratio of cathodic to anodic peak areas

AN -   Acetonitrile
BL -   Butyrolactone
DMF -   Dimethylformamide
PC -   Propylene carbonate

TABLE XII

SYSTEMS EXHIBITING ANODIC PEAK ONLY *

System	CV	Peak Current Density Range
Cu/DMF-LiCl (2.5 m)	2579	high
CuF_2/DMF-KPF_6 (2.0 m)	2615	medium low
CuF_2/DMF-KPF_6 (1.0 m)	2620	medium low
Ni/DMF-$LiPF_6$	2778	high
Ni/PC-$LiPF_6$	2701 (a)	low
Co/AN-KPF_6 (b)	2567	high
Mo/DMF-$Mg(ClO_4)_2$	2856	medium high
Mo/PC-$Mg(ClO_4)_2$	2870	low
In/DMF-$MgCl_2$	2883	very high
Fe/DMF-$AlCl_3$+LiCl	2848	very high
Fe/DMF-$LiClO_4$	2937 (a)	high
Fe/DMF-$Mg(ClO_4)_2$	2858	medium low
Fe/PC-$Mg(ClO_4)_2$	2863 (a)	low
Fe/PC-KPF_6	2893	high

*   -   Maximum cathodic current density in very low range (<1 ma/cm^2) unless otherwise noted

(a)   -   Low range cathodic (<10 ma/cm^2)

(b)   -   Containing 500 ppm water

AN   -   Acetonitrile
BL   -   Butyrolactone
DMF -   Dimethylformamide
PC   -   Propylene carbonate

TABLE XIII

SYSTEMS EXHIBITING CATHODIC PEAK ONLY

System	CV	Peak C. D. Range
Ag/DMF-LiPF$_6$	2723	low

TABLE XIV

SYSTEMS EXHIBITING NO PEAKS

System	CV
Mo/DMF-AlCl$_3$+LiCl	2837
Mo/DMF-LiCl (0.5 m)	2907
Mo/DMF-LiClO$_4$ (1.0 m)	2932
Mo/DMF-MgCl$_2$	2882
Mo/DMF-KPF$_6$ (0.75 m)	2943
Mo/PC-LiClO$_4$	2917
Mo/PC-KPF$_6$	2898
Fe/DMF-MgCl$_2$	2877
Fe/DMF-KPF$_6$ (0.75 m)	2948
Fe/PC-LiClO$_4$	2922

DMF -   Dimethylformamide
PC   -   Propylene carbonate

II. REFERENCES

1. Whittaker Corporation, Narmco Research and Development Division, NASA Contract NAS 3-8509, First Quarterly Report, NASA Report CR-72069, August 1966.

2. Whittaker Corporation, Narmco Research and Development Division, NASA Contract NAS 3-8509, Second Quarterly Report, NASA Report CR-72138, November 1966.

3. Whittaker Corporation, Narmco Research and Development Division, NAS Contract NAS 3-8509, Third Quarterly Report, NASA Report CR-72181, February 1967.

4. Whittaker Corporation, Narmco Research and Development Division, NASA Contract NAS 3-8509, Fourth Quarterly Report, NASA Report CR-72256, April 1967.